ARTICLE

ACS chemical biology

Water-Soluble Triarylphosphines as Biomarkers for Protein *S*-Nitrosation

Erika Bechtold[†], Julie A. Reisz[†], Chananat Klomsiri[‡], Allen W. Tsang[§], Marcus W. Wright[†], Leslie B. Poole[‡], Cristina M. Furdui[§], and S. Bruce King[†,*]

[†]Department of Chemistry, Wake Forest University, Winston-Salem, North Carolina 27109, [‡]Center for Structural Biology, Department of Biochemistry, [§]Department of Molecular Medicine, Wake Forest University School of Medicine, Winston-Salem, North Carolina 27157

ABSTRACT *S*-Nitrosothiols (RSNOs) represent an important class of post-translational modifications that preserve and amplify the actions of nitric oxide and regulate enzyme activity. Several regulatory proteins are now verified targets of cellular *S*-nitrosation, and the direct detection of *S*-nitrosated residues in proteins has become essential to better understand RSNO-mediated signaling. Current RSNO detection depends on indirect assays that limit their overall specificity and reliability. Herein, we report the reaction of *S*-nitrosated cysteine, glutathione, and a mutated C165S alkyl hydroperoxide reductase with the water-soluble phosphine tris(4,6-dimethyl-3-sulfonatophenyl)phosphine trisodium salt hydrate (TXPTS). A combination of NMR and MS techniques reveals that these reactions produce covalent *S*-alkylphosphonium ion adducts (with $S-P^+$ connectivity), TXPTS oxide, and a TXPTS-derived aza-ylide. Mechanistically, this reaction may proceed through an *S*-substituted aza-ylide or the direct displacement of nitroxyl from the RSNO group. This work provides a new means for detecting and quantifying *S*-nitrosated species in solution and suggests that phosphines may be useful tools for understanding the complex physiological roles of *S*-nitrosation and its implications in cell signaling and homeostasis.

Reactive oxygen and nitrogen species (ROS/RNS) affect cellular signaling processes at concentrations far below those required to inflict oxidative damage (*1–4*). The overoxidation and metabolism of nitric oxide (NO), an endogenous cell signaling agent, produces several RNSs including nitrogen dioxide and nitrite, which can generate competent nitrosation agents (*5, 6*). Nitrosation of cysteine sites yields *S*-nitrosothiols (RSNOs) that preserve, modulate, and amplify the actions of NO. This selective and reversible process represents an important post-translational modification in cell signaling and regulation (*3, 6–8*). Several proteins have been identified as targets of cellular *S*-nitrosation including glyceraldehyde-3-phosphate dehydrogenase (GAPDH), papain, hemoglobin (Hb), and several caspases (*5, 9–12*). Inflammatory stimuli, including RNS, increase overall cellular RSNO formation, which further mediates the inflammatory process (*9, 13–17*). Direct detection and specific identification of *S*-nitrosated residues in proteins is essential to better understand RSNO-mediated signaling. Current techniques, such as the biotin switch assay, Saville assay, and chemiluminescence-based methods, are indirect methods of detection (*18–23*). Also, variability in these assays has challenged their accuracy and driven the search for alternative detection systems (*24, 25*). Deciphering the role and importance of RSNOs in biology requires direct and specific methods of quantification. We report a new strategy to covalently label biological RSNOs using the water-soluble phosphine tris(4,6-dimethyl-3-sulfonatophenyl) phosphine trisodium salt hydrate (TXPTS, Scheme 1) (*26*).

Earlier work showed that the reaction of trityl-*S*-nitrosothiol with triphenylphosphine yields an *S*-substituted aza-ylide (**1**, Scheme 1) and provided in-

***Corresponding author,** kingsb@wfu.edu.

Received for review November 30, 2009 and accepted February 10, 2010.

Published online February 10, 2010

10.1021/cb900302u

Scheme 1. Reactions of triarylphosphines with *S*-nitrosothiols in organic and aqueous systems

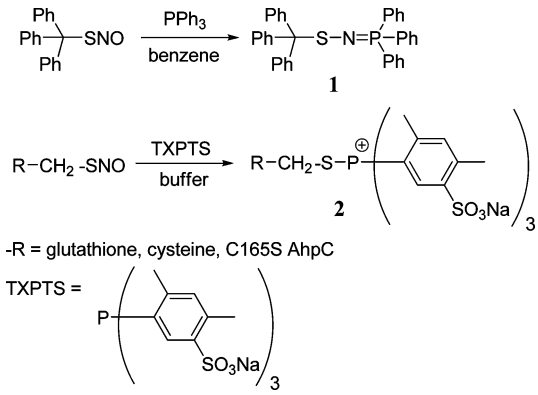

spiration for developing an SNO-specific label (*27*). Recently, Xian revealed that the treatment of various organic SNOs with derivatized triarylphosphines provides products arising from similar *S*-substituted aza-ylides (*28–30*). In the presence of properly situated electrophiles on the triarylphosphine, the *S*-substituted aza-ylide intermediates undergo ligation to form stable sulfenamides or disulfide iminophosphoranes (*28–30*). Treatment of *S*-nitrosocysteine ester derivatives with various phosphines yields the corresponding dehydroalanines through intramolecular elimination *via* a similar *S*-substituted aza-ylide (*28*). These results encouraged our use of the water-soluble phosphine TXPTS as a potential RSNO trap. We report the reactions of TXPTS with *S*-nitrosocysteine (Cys-SNO), *S*-nitrosoglutathione (GSNO), and a mutated peroxiredoxin, *S*-nitrosated C165S alkyl hydroperoxide reductase (C165S AhpC-SNO) to yield the covalent *S*-alkylphosphonium salt (**2**, Scheme 1).

RESULTS AND DISCUSSION

Haake's observation that the reaction of trityl *S*-nitrosothiol and triphenylphosphine gives an *S*-substituted aza-ylide (**1**, Scheme 1) reveals that organic *S*-nitrosothiols can act in a similar manner as the organic azide in Staudinger-type reductions/ligations (*27, 31*). On the basis of this work, we hypothesized that protein and other biologically relevant *S*-nitrosothiols could potentially be labeled as structurally unique *S*-substituted aza-ylides through their reaction with the water-soluble triarylphosphine (TXPTS). Recent work by Xian shows that a variety of *S*-nitrosothiols react with triaryl and trialkylphosphines to give *S*-substiuted aza-ylides, which undergo further reactions to yield a variety of different products depending on both RSNO and phosphine structure (*29, 30*). In the presence of an electrophilic trap, these *S*-substituted aza-ylide intermediates ligate to generate sulfenamides or rearrange to disulfide iminophosphoranes (*29, 30*). In the absence of an electrophilic trap, the intermediate *S*-substituted aza-ylide eliminates to form dehydroalanine-containing products (*28*). This work reveals rich reaction chemistry between *S*-nitrosothiols and phosphines that may form the basis of new labeling methods, but in general, these processes have been limited to protected versions of cysteine and glutathione in organic or organic/buffer mixtures. Using a combination of NMR- and MS-based techniques, we sought to critically evaluate the reaction between TXPTS and several physiologically relevant *S*-nitrosothiols. We report that the reactions between *S*-nitrosothiols of cysteine, glutathione, and a mutant of the bacterial peroxiredoxin, AhpC, with the water-soluble triarylphosphine (TXPTS) yield a unique set of products that include TXPTS oxide (**3**), the stable aza-ylide of TXPTS (**4**), and an *S*-alkylphosphonium adduct (RS-P^+ connection, **5** and **6**, Schemes 2 and 3).

Reaction of Triphenylphosphine with Trityl *S*-Nitrosothiol. Treatment of trityl *S*-nitrosothiol with 2 equiv of triphenylphosphine in benzene yields the *S*-substituted aza-ylide (**1**, 92% yield, Scheme 1), which corroborates previous results and provides the first X-ray crystallographic and ^{31}P NMR characterization of this compound (see Supporting Information).

Reaction of TXPTS and *S*-Nitrosoglutathione (GSNO). The reaction of TXPTS and *S*-nitrosoglutathione (GSNO, a commercially available or readily prepared stable pink solid) offers an opportunity to evaluate the formation of *S*-substituted aza-ylides in water or buffer. UV−vis spectroscopy shows the rapid loss of the *S*-nitrosothiol functional group in GSNO upon addition of TXPTS as evidenced by the decrease in absorbance at 545 nm (Supporting Information). ^{31}P NMR spectroscopy provides detailed information regarding this reaction. A mixture of products results when freshly prepared GSNO (1 equiv) and TXPTS (2 equiv) are combined in buffer (50 mM HEPES, 1 mM DTPA, pH 7.1) in the dark.

SCHEME 2. Reaction of TXPTS with *S*-nitrosoglutathione at pH 7

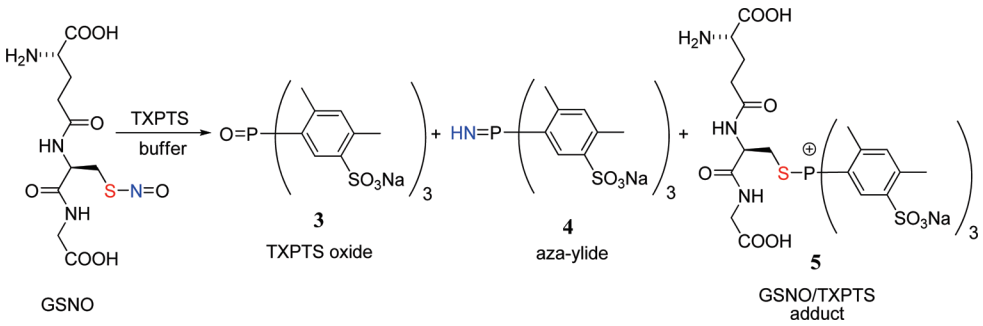

The peak for phosphine ($\delta = -28.8$ ppm) decreases with time, and three new peaks at $\delta = 34.5$, 39.7, and 47.2 ppm emerge over 30 min (Figure 1). No other phosphorus-derived species are observed on this time scale, and control experiments show that TXPTS does not react with GSH and only to a small extent (~3%) with GSSG to form the same product with the resonance at 47.2 ppm as judged by ^{31}P NMR (Supporting Information). Comparison to known standards allows identification of the peak at 39.7 ppm as TXPTS oxide (**3**, Scheme 2) and the peak at 34.5 ppm as the TXPTS-derived ylide (**4**, Scheme 2). Monitoring this reaction mixture over time shows the immediate formation of the species at 47.2 ppm, whereas **3** and **4** emerge more gradually over the course of 2 h (Figure 2). Integration of the ^{31}P NMR spectrum after 1 h indicates the formation of these three products in roughly a 1:1:1 ratio, which gives an estimated yield of 67% for **5** (based on starting GSNO). The use of ^{15}N-labeled GSNO results in an apparent coupling ($^{1}J_{N-P} = 23$ Hz) in the peak at 34.5 ppm, which corresponds to **4**, but not in any of the other peaks. This observed splitting varies over time, suggesting some dynamic changes of **4** under these conditions (possibly water addition to the ylide). Treatment of this reaction mixture with dithiothreitol regenerates TXPTS ($\delta = -28.8$ ppm) at the expense of the species at 47.2 ppm with no change in the peaks that correspond to **3** and **4** (Supporting Information). The addition of a sodium hydroxide solution to the reaction mixture results in the disappearance of the peaks at 34.5 and 47.2 ppm and an increase in phosphine oxide (**3**, 39.7 ppm). The ^{13}C and ^{1}H NMR spectra of this reaction show complicated mixtures that do not allow for the clear identification of the phosphorus-containing species responsible for the resonance at 47.5 ppm or definitive estimates of the total product yields. Gas chromatographic headspace analysis and chemiluminescence nitric oxide detection reveal that no nitrous oxide (evidence for HNO) and only a trace amount of nitric oxide form during the reaction of TXPTS and GSNO.

Liquid chromatography–mass spectrometry (LC–MS) further confirms the identity of these products and provides insight into the structure of the compound responsible for the peak at 47.2 ppm in the ^{31}P NMR spectrum. Analysis of the GSNO/TXPTS reaction mixture validates the formation of **3** and **4** given their comparison to known standards (Supporting Information). The observed *m*/*z* of the final compound (892.1) suggests an adduct of GSNO and TXPTS with the loss of NO as opposed to the initially predicted -S-N=PR_3 motif leading to the proposal of an *S*-alkylphosphonium product (**5**, Scheme 2) (*27–30*). The use of ^{15}N-labeled GSNO results in the formation of ^{15}N-labeled **4** indicating the transfer of the -S-N=O nitrogen atom to the phosphorus atom of TXPTS (Supporting Information). Similar LC–MS experiments do not support the formation of GSH or GSSG during this reaction.

A series of 2-D NMR experiments confirm the proposed S–P^+ bonding motif of **5**. A ^{1}H–^{31}P COSY indi-

SCHEME 3. Reaction of TXPTS with *S*-nitrosocysteine at pH 7

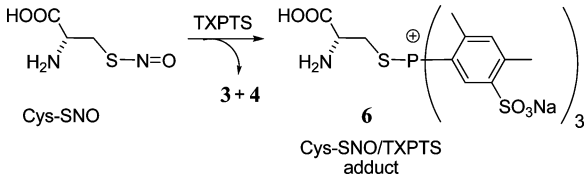

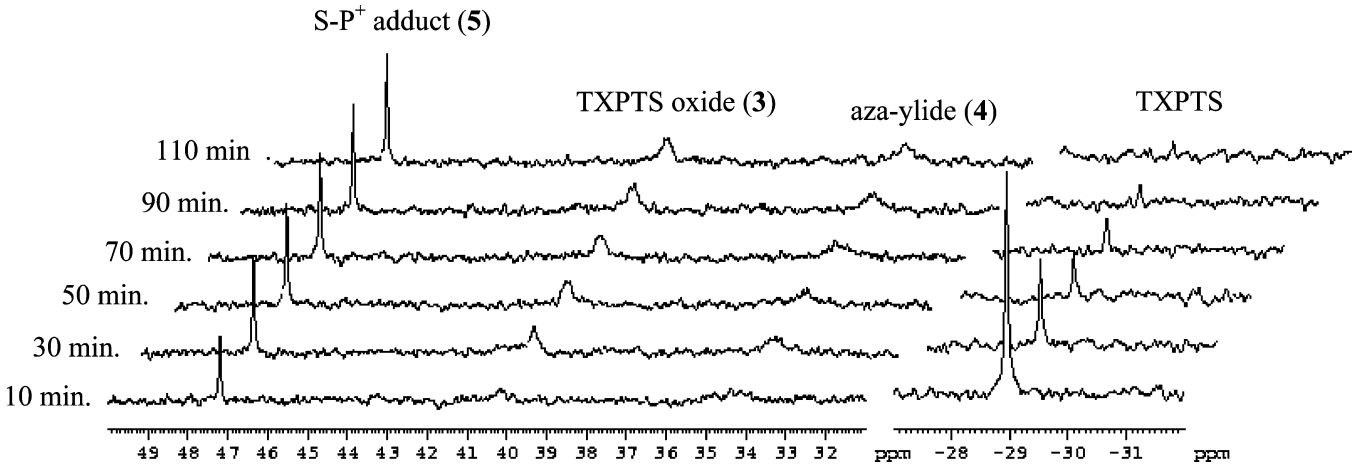

Figure 1. ^{31}P NMR time course experiment of the GSNO and TXPTS reaction. ^{15}N-GSNO (1 equiv) and TXPTS (2 equiv) were incubated in a HEPES/DTPA buffered solution (pH 7.1) with 10% D_2O, and the reaction was monitored using ^{31}P NMR with 1 scan every 20 min. The peaks at 47.2, 39.7, and 34.5 ppm correspond to 5, 3, and 4, respectively, and TXPTS starting material at −28.8 ppm. All peaks were referenced to a 3% H_3PO_4 ($\delta = 0$ ppm) external standard, which was omitted for clarity.

cates that the ^{31}P signal of **5** (47.2 ppm) correlates to three protons in the ^1H NMR spectrum (3.85, 3.42, and 3.01 ppm, presumably the -CH and diastereotopic -CH_2 of the cysteine side chain of **5**), in the reaction mixture (Figure 2, panel A). Using this obtained ^1H correlation, the $^1H-^{13}C$ HMQC of the same reaction mixture reveals the proximity of the P atom of the $S-P^+$ moiety to nearby -CH_2 and -CH carbons. Coupling constant analysis shows splitting of the -CH_2 carbon ($^2J_{P-C} = 14.6$ Hz, Figure 2, panel B), providing evidence for attachment of the phosphine through an $S-P^+$ linkage.

Reaction of TXPTS and *S*-Nitroso-L-cysteine (Cys-SNO). Similar ^{31}P NMR experiments show the formation of three phosphorus-derived products from the mixture of freshly prepared Cys-SNO (1 equiv) with TXPTS (2 equiv) in buffer (50 mM HEPES, 1 mM DTPA, pH 7.1) in the dark that correspond to TXPTS oxide (**3**, $\delta =$ 39.7 ppm), the TXPTS-derived ylide (**4**, $\delta = 34.5$), and a

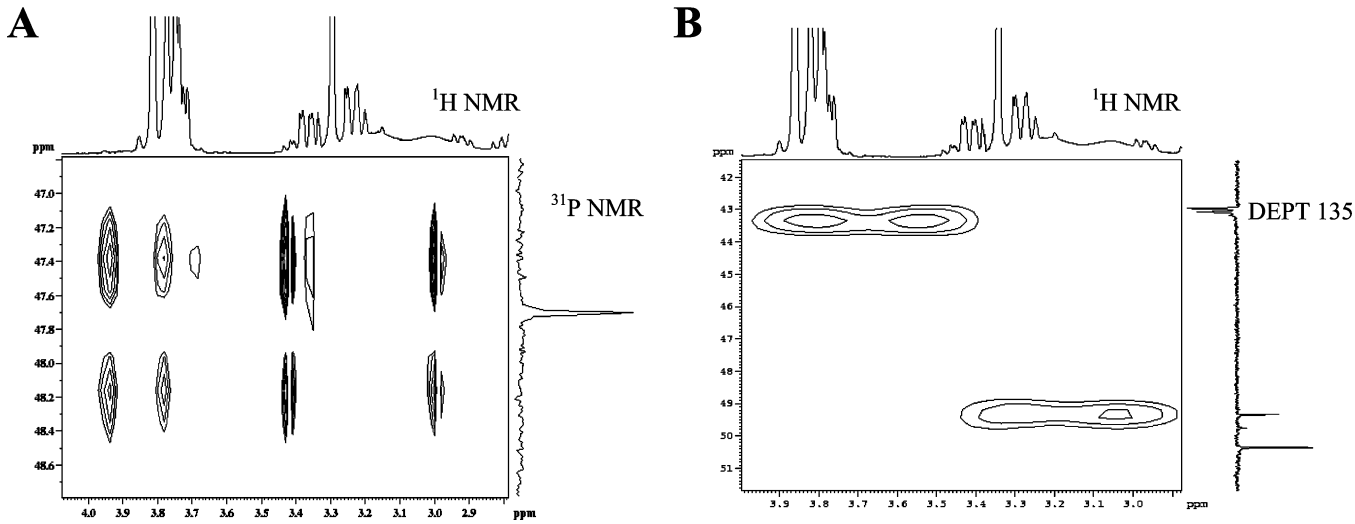

Figure 2. 2-D NMR of the GSNO and TXPTS reaction. a) $^1H-^{31}P$ COSY of the GSNO/TXPTS reaction mixture in D_2O. b) $^1H-^{13}C$ HMQC of the GSNO/TXPTS reaction mixture in D_2O

presumed cysteine-derived *S*-alkylphosphonium adduct (**6**, Scheme 3, $\delta = 46.1$ ppm) after 30 min (Supporting Information). No other phosphorus-derived species were observed, and control experiments show that TXPTS does not react with cysteine but partially reacts with cystine to form the same product with a resonance at 46.1 ppm (~15%, Supporting Information), indicating that TXPTS may react with certain disulfides. Integration of the ^{31}P NMR spectrum after 1 h indicates the formation of compounds **3**:**4**:**6** in roughly a 3:1:1 ratio, which suggests a more rapid hydrolysis of **6** compared to **5**. Analogous to the GSNO reaction, treatment of this mixture with dithiothreitol regenerates TXPTS ($\delta = -28.8$ ppm) at the expense of the species at 46.1 ppm with no change in the peaks that correspond to **3** and **4** (Supporting Information). LC−MS analysis of the Cys-SNO/TXPTS mixture also confirms the presence of **3** and **4**, as well as the expected mass for the S−P$^+$ adduct **6** (Supporting Information).

The commercial availability of (3-^{13}C)-Cys provides the opportunity to further confirm the structure of the S−P$^+$ adduct (**6**) in solution. Treatment of (3-^{13}C)-Cys-SNO with TXPTS followed by ^{31}P NMR spectroscopy showed through-bond coupling of the ^{31}P atom to the ^{13}C with an observed $^2J_{C-P}$ coupling = 3.7 Hz, which confirms the connectivity and covalent nature of the *S*-alkylphosphonium adduct (**6**, Supporting Information). Importantly, LC−MS analysis revealed a 1 amu increase in mass for the S−P$^+$ species (**6**), further validating the covalent attachment of TXPTS in the adduct (Supporting Information). The ^{13}C NMR spectrum of the reaction between TXPTS and (3-^{13}C)-Cys-SNO shows the presence of four peaks at 42.1, 42.4, 60.8, and 62.7 ppm (Supporting Information). The resonance at 42.1 ppm is a doublet ($^2J_{P-C} = 8.6$ Hz), indicating coupling and further corroborating the ^{31}P NMR results. Comparison to standards reveals that the peak at 60.8 ppm corresponds to the methylene carbon of L-serine. The other two resonances (42.4 and 62.7 ppm) currently remain unidentified but appear during the preparation of Cys-SNO (Supporting Information). This spectrum also indicates the absence of cysteine, cystine, and dehydroalanine (no resonances between 100−150 ppm) in the reaction mixture, in contrast to recent work that shows dehydroalanine formation in the reaction of Cys-SNO derivatives with phosphines (*28*).

While providing strong evidence of *S*-alkylphosphonium ion formation, the identification of other nonphosphorus containing products (by NMR) and our inability to completely account for the GSNO and Cys-SNO reveal the complexity of these reactions. Both NMR and LC−MS examination of these reaction mixtures do not show the presence of disulfides (GSSG/cystine) or the glutathione-derived sulfenamide ($GSNH_2$) and only small amounts of thiol (GSH/cysteine), eliminating these likely products. The identification of serine from the reaction of Cys-SNO, which may form from the hydrolysis of **6**, demonstrates the complexity of these reactions. These results indicate the likelihood of other processes during *S*-alkylphosphonium ion formation and breakdown that may include reactions of sulfenamide intermediates, other rearrangements/dehydrations of intermediate aza-ylides, and various reactions of the *S*-alkylphosphonium ions (**5** and **6**).

Literature values for *S*-alkylphosphonium ion ^{31}P NMR shifts are roughly 40−50 ppm, consistent with the observed resonances for **5** and **6** (*32*–*34*). These SP$^+$ ions also represent known intermediates in phosphine-mediated disulfide reductions. In general, phosphines, including tris(2-carboxyethyl)phosphine (TCEP), the reagent of choice for protein disulfide reduction, rapidly reduce disulfides to the *S*-alkylphosphonium intermediate that hydrolyzes to give free thiol and phosphine oxide (*35*–*38*). Control experiments show that TXPTS reacts with GSSG and cystine to a limited extent to yield the S−P$^+$ intermediates (**5** and **6**). The unique structure of TXPTS appears to slow the hydrolysis of these SP$^+$ species, allowing them to be isolated. The steric effects of the functionalized phenyl rings may hinder nucleophilic attack by water, and furthermore, the electron-donating ability of the *ortho* and *para* methyl substituents on TXPTS likely increases the electron density at phosphorus, reducing electrophilicity and retarding attack by water or other nucleophiles. Once formed, compounds **5** and **6** react with thiols to yield the phosphine and hydrolyze in base to the give the phosphine oxide, consistent with known reactivity of *S*-alkylphosphonium ions.

Reaction of TXPTS with AhpC-SNO. Given the reproducible formation of *S*-alkylphosphonium adducts from the reactions of TXPTS with GSNO and Cys-SNO, we examined the reaction of the *S*-nitrosated peroxiredoxin mutant C165S alkyl hydroperoxide reductase C (AhpC-SNO) with TXPTS. This mutant was an ideal candidate for examining the interaction of a protein SNO with TXPTS since the remaining active site cysteine (Cys46) is sus-

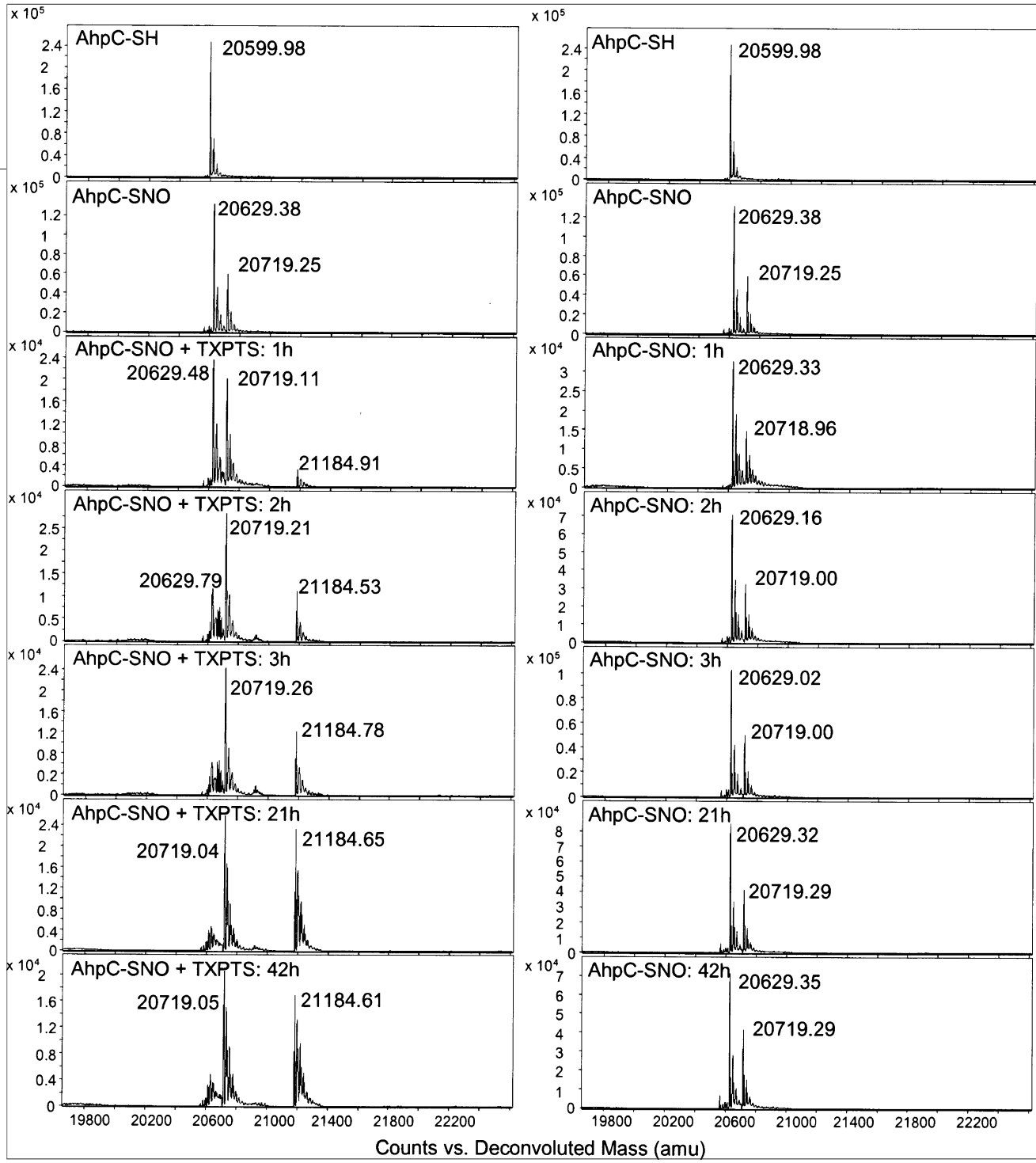

Figure 3. ESI-TOF-MS data showing TXPTS covalently labeling the *S*-nitrosated mutated peroxiredoxin (C165S AhpC-SNO). The exact mass of the covalent adduct is 21184.69; MW of the AhpC-SNO is 20629.55. The MW 20719.14 corresponds to the mixed disulfide that forms between AhpC-SNO and Cys-SNO (AhpC-S-S-Cys). (left) C165S AhpC-SNO with 25-fold excess TXPTS over 42 h. (right) Control showing C165S AhpC-SNO in the absence of TXPTS under the same conditions.

ceptible to oxidative modifications, including sulfenic acid and *S*-nitrosothiol formation (*39*). Incubation of freshly prepared AhpC-SNO with a 25-fold excess of TXPTS in buffer (50 mM HEPES, 1 mM DTPA) at 25 °C forms an *S*-alkylphosphonium (SP^+-type) adduct over several hours (Figure 3) as shown by electrospray ionization-time-of-flight (ESI-TOF) MS experiments. As seen in Figure 3, both AhpC-SNO (exact mass = 20629.38) and the *S*-thiolation product with cysteine (AhpC-S-S-Cys, exact mass = 20719.11) form upon mixture of AhpC (reduced) and Cys-SNO. Upon incubation of this sample with TXPTS, a time-dependent decrease of AhpC-SNO occurs with the emergence of the corresponding AhpC-SP^+ adduct (exact mass = 21184.69)

SCHEME 4. Proposed mechanism for the formation of the S-N═P type aza-ylide (1)

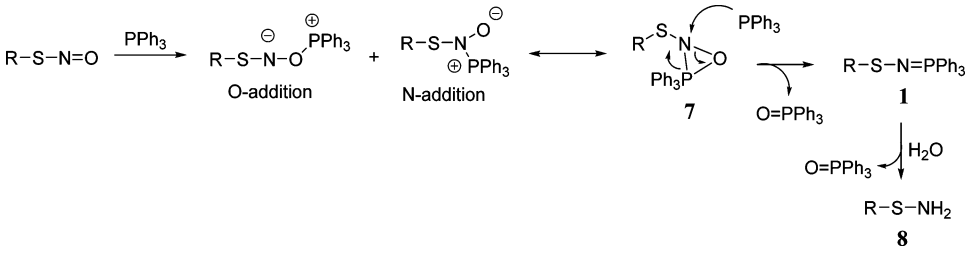

was formed in roughly 83% yield after 3 h as estimated by the relative intensities (Figure 3). Based on the *m*/*z* difference of 555.1 amu and the lack of reaction between AhpC (reduced) and TXPTS, the phosphine (exact mass = 652 as the trisodium salt) appears to be covalently bound to the protein in an S−P$^+$ fashion. Direct treatment of the free thiol form of C165S AhpC (AhpC-SH) with TXPTS does not form this product by ESI-TOF MS (Supporting Information). Figure 3 also indicates that TXPTS does not react with the AhpC-S-S-Cys mixed disulfide over 42 h. The AhpC-derived S−P$^+$ species demonstrates excellent stability over several days at RT and under denaturing conditions (40% acetonitrile, Supporting Information).

To the best of our knowledge, these results describe the first covalent labeling of an *S*-nitrosated protein in buffer and demonstrate the potential of phosphines as protein SNO labels. While TXPTS rapidly reacts with small molecule RSNOs, Figure 3 shows that the reaction with AhpC-SNO occurs much more slowly. Steric differences in the environment of the -SNO group likely dictate the rates of these reactions, and thus rates may vary among proteins with different thiol accessibility; the cysteine of AhpC has been shown to react relatively sluggishly with alkylating agents (*40*). Evaluation of the rate and selectivity of this reaction with protein SNOs and other oxidized sulfur species is warranted and will be required for the development of this reagent as a labeling tool.

Evaluating the Mechanism of SNO-Derived Adduct Formation. Scheme 4 depicts a proposed mechanism for the formation of *S*-substituted aza-ylides from an *S*-nitrosothiol with a triarylphosphine. This reaction could yield products through phosphorus-addition to either nitrogen or oxygen, and both could exist as a three-membered ring (**7**, Scheme 4) (*27, 30*). Addition of a second phosphine to **7** (or one of the initial addition products) would give the phosphine oxide and *S*-substituted aza-ylide in equal proportions (as observed for **1**, Scheme 1) (*27*).

SCHEME 5. Two proposed mechanisms for the formation of an SNO-derived adduct from TXPTS

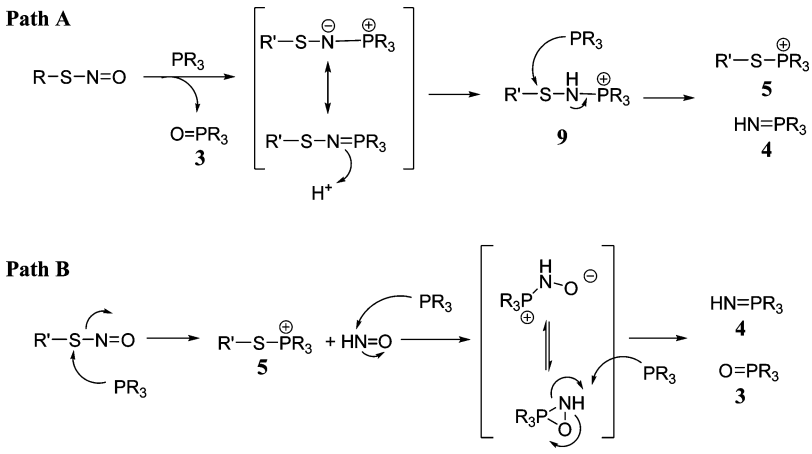

The described spectroscopic and LC−MS studies show that the reaction of GSNO or Cys-SNO with TXPTS in buffer rapidly consumes the *S*-nitrosothiol. While ^{31}P NMR provides evidence of TXPTS phosphine oxide (**3**) formation as expected, ^{31}P NMR chemical shift comparison to **1**, the lack of observed splitting in the

^{31}P NMR spectrum in the reaction using ^{15}N-GSNO and LC−MS work do not support formation of the expected *S*-substituted aza-ylide. Hydrolysis of any *S*-substituted aza-ylide product to the corresponding sulfenamide ($RSNH_2$, **8**, Scheme 4) and **3** would explain the absence of the *S*-substituted aza-ylide, but the ^{31}P NMR identification of two other phosphorus-containing species clearly indicates a different mechanism; direct formation of the *S*-substituted aza-ylide followed by hydrolysis would produce phosphine oxide (**3**) as the only phosphorus containing product. This work identifies the two other phosphorus-containing products as the aza-ylide (**4**) and the corresponding *S*-alkylphosphonium salts (**5**−**6**, Schemes 2 and 3). Aza-ylide (**4**), which has been characterized during the reaction of TXPTS and nitroxyl (HNO), demonstrates considerable water stability, presumably due to stabilization of the phosphonium ion by the electron-donating ortho and para methyl groups of TXPTS (*41*). The reaction of TXPTS with ^{15}N-labled GSNO results in ^{15}N incorporation in **4** and reveals the formal 6 e^- reduction of the *S*-nitrosothiol nitrogen atom to ammonia (consistent with the absence of NO/HNO formation). This reaction finds some precedence in the GSNO reductase (aka alcohol dehydrogenase)-mediated reduction of GSNO to ammonia (*42, 43*).

Scheme 5 shows two potential mechanisms that account for the observed phosphorus-containing products. Path A proceeds through a mechanism that includes an *S*-substituted aza-ylide (-S-N═P), presumably formed through a mechanism as seen in Scheme 4. In aqueous conditions, protonation of this *S*-substituted aza-ylide gives a new intermediate (**9**) that rapidly reacts with another equivalent of phosphine to simultaneously yield equal amounts of the *S*-alkylphosphonium ion (**5** or **6**) and the aza-ylide (**4**). This mechanism utilizes 3 equiv of phosphine and predicts a 1:1:1 ratio of **3**:**4**:**5**, as experimentally observed for the GSNO reaction. While 2 equiv of phosphine were used in these experiments, the inherent instability of GSNO provided for excess phosphine during the reaction. The lack of experimental evidence of an *S*-subsituted aza-ylide (**1**) and previous work showing that TXPTS reacts with HNO to form equal amounts of **3** and **4** suggest a more direct mechanism for observed product formation (*41*). Path B (Scheme 5) depicts the direct nucleophilic attack of TXPTS on the sulfur atom of an *S*-nitrosothiol to form the *S*-alkylphosphonium ion (**5**, for GSNO) with release of HNO. The reaction of 2 equiv of TXPTS with nascent HNO would yield **3** and **4**. This mechanism also requires 3 equiv of phosphine and predicts a 1:1:1 ratio of **3**:**4**:**5**. The ^{31}P NMR time-course experiment (Figure 2) supports Path B with the rapid initial formation of **5** followed by the emergence of **3** and **4**, whereas Path A would initially produce **3** followed by **4** and **5**. Given the rapid reaction of TXPTS and HNO, the failure to detect N_2O (the HNO dimerization/dehydration product) does not eliminate Path B. While both mechanisms account for the observed products and ratios, further experiments, particularly a detailed kinetic analysis of the constituent reactions of this sequence, are required to delineate the mechanisms.

In summary, the triarylphosphine TXPTS reacts directly with *S*-nitrosothiol residues to produce stable *S*-alkylphosphonium ions (**5**, **6**, or AhpC-SP^+) as well as TXPTS oxide (**3**) and the TXPTS-derived aza-ylide (**4**), This work details the first reaction of triarylphosphines with RSNOs in water. Mechanistically, this reaction may proceed through an *S*-substituted aza-ylide or through the direct displacement of HNO from the RSNO group. This reaction, which is amenable to MS detection and ^{31}P NMR spectroscopy, provides a new method for identifying *S*-nitrosated species in solution. This unique reactivity suggests that phosphines may be useful tools for understanding the complex physiological roles of biological *S*-nitrosation and its implications in cell signaling and homeostasis.

METHODS

Tris(4,6-dimethyl-3-sulfonatophenyl)phosphine trisodium salt hydrate (TXPTS) was purchased from Strem Chemicals. Glutathione (reduced and oxidized), L-cysteine, L-cystine, 1,4-dithiothreitol, sodium nitrite, sodium hydroxide, triphenylphosphine, triphenylmethane thiol, butyl nitrite, hydrogen peroxide solution (10 M), deuterium oxide, and deuterated chloroform were purchased from Sigma Aldrich. Hydrochloric acid solution (1 N) was purchased from TCI. (3-^{13}C)-L-Cysteine and ^{15}N-sodium nitrite were purchased from Cambridge Isotope Laboratory. All reagents were used directly from suppliers without further purification.

Preparation of *S*-Substituted Aza-ylide (1). A solution of trityl thionitrite in $CHCl_3$ (0.1905 g, 0.62 mmol, (λ_{max} ($CHCl_3$) 335, 545 nm) (*44*) was added to a solution of triphenylphosphine (0.33 g, 1.25 mmol) in anhydrous benzene (5 mL) at RT. After 30 min, the solids were filtered to give **1** as a bright yellow solid

(*27*). Recrystallization in CH_3CN/toluene afforded **1** as bright yellow crystals. ^{31}P NMR (121 MHz, $CDCl_3$) δ 17.3.

Preparation of *S*-Nitrosocysteine (Cys-SNO). A solution of L-cysteine (0.06 g, 0.34 mmol) in 0.75 N HCl (4 mL) with 15 mM EDTA was added to a solution of sodium nitrite (0.035 g, 0.5 mmol) in H_2O (5 mL) with 0.5 mM EDTA at 4 °C. After 10 min, the reaction turned deep red and was neutralized with 1 N NaOH (2.5 mL) to afford a solution of L-Cys-SNO (H_2O, ε_{335nm} 503 M^{-1} cm^{-1}). (3-^{13}C)-L-Cys-SNO was made using the same procedure. (^{15}N)-*S*-Nitrosocysteine was prepared using ^{15}N-sodium nitrite.

Preparation of *S*-Nitrosoglutathione (GSNO). (*45*)Sodium nitrite (0.345 g, 5 mmol) was added to an ice-cold solution of glutathione (1.53 g, 5 mmol) in 2 N HCl (5 mL). After 40 min at 4 °C, the red solution was treated with acetone (10 mL) and stirred for an additional 10 min. The resulting pink solid was filtered off and washed successively with ice-cold water (5 mL), acetone (3 mL), and ether (3 mL) to afford *S*-nitrosoglutathione (1.29 g, 76%) (H_2O, ε_{335nm} 922 M^{-1} cm^{-1}, ε_{545nm} 15.9 M^{-1} cm^{-1}). (^{15}N)-*S*-Nitrosoglutathione was prepared using ^{15}N-sodium nitrite.

Preparation of *S*-Nitroso (C165S) AhpC. The mutant form of *Salmonella typhimurium* AhpC, C165S, was overexpressed and purified from *Escherichia coli* as previously described (*40, 46*). A solution of reduced protein (0.5 mg mL^{-1}, 500 μL) in HEPES (50 mM), DTPA (1 mM) buffer (pH 7.1) was incubated with freshly prepared *S*-nitrosocysteine (1 mM) at 25 °C for 60 min in the dark. Removal of *S*-nitrosocysteine was performed using BioRad spin columns with Bio-Gel P6 equilibrated in HEPES (50 mM), DTPA (1 mM) buffer (pH 7.1). The formation of C165S AhpC-SNO (as well as a lesser amount of C165S AhpC/Cys mixed disulfide) was monitored by ESI-TOF MS as described below.

Labeling of AhpC-SNO Using TXPTS. A solution of TXPTS (2 μL, 250 mM) was added to a solution of freshly prepared AhpC-SNO (200 μL, 100 μM) in HEPES (50 mM), DTPA (1 mM) buffer. Aliquots (50 μL) were taken at different time points and diluted with ammonium bicarbonate buffer (50 μL, 50 mM, pH 7.5), then TXPTS was removed using BioRad spin columns packed with Bio-Gel P6 (BioRad), and samples were equilibrated with ammonium bicarbonate buffer (50 mM, pH 7.5). The samples were analyzed by ESI-TOF MS as described below.

NMR Analysis. *1-D Analyses.* ^1H NMR spectra were recorded on Bruker Avance DPX-300 and DRX-500 instruments at 300.13 and 500.13 MHz, respectively. ^{13}C and DEPT NMR spectra were recorded on a Bruker DRX-500 instrument operating at 125.76 MHz. ^{31}P NMR spectra were recorded on Bruker DPX-300 and DRX-500 instruments operating at 121.49 and 202.46 MHz, respectively, and ^{31}P chemical shifts are relative to 3% H_3PO_4 (δ = 0 ppm) contained in a concentric internal capillary (Wilmad).

2-D Analyses. The $^1H-^{31}P$ gradient selected COSY spectrum was acquired with 2048 complex points in t_2, 256 points in t_1, and 40 transients with a pulse repetition delay of 2 s. A sweep width of 10 ppm in ^1H (centered at 4.5 ppm) and 100 ppm in ^{31}P (centered at 10 ppm) was used. Data sets were multiplied with 90° phase shifted squared-sinebell apodization function and zero-filled to 512 × 512 data points before Fourier transformation. Chemical shifts were referenced to the residual H_2O signal and the observed SP^+ chemical shift (^{31}P NMR shift of 47.7 ppm). The 2-D HMQC spectrum was collected with 256 complex points in t_2, 256 points in t_1, and 32 transients with a pulse repetition delay of 1.5s. A sweep width of 7.78 ppm in ^1H (centered at 5 ppm) and 250 ppm in ^{13}C (centered at 110 ppm) was used. Data sets were multiplied with 90° phase shifted squared-sinebell apodization function and zero-filled to 1024 × 1024 data points before Fourier transformation.

LC–MS Analysis. LC–MS experiments were performed on an Agilent Technologies 1100 LC/MSD Trap instrument. Separations were achieved using an Agilent Zorbax Rapid Resolution SB-C18 reverse phase column (2.1 mm × 30 mm/3.5 μm) at 25 °C with solvent A = 0.1% ammonium formate in water and solvent B = HPLC-grade acetonitrile. Flow rate: 0.4 mL min^{-1}. Gradient for conditioning of column: 100% B to 15% B over 90 min. Gradient for GSNO + TXPTS analyses: 1% B for 1 min, ramp to 3% B over 2 min, ramp to 5% B over 3 min, and hold for 1 min, for a total run time of 7 min. The postrun time was 3 min at 5% B. Gradient for Cys-SNO + TXPTS analyses: 3% B for 3 min, ramp to 10% B for 3 min, and lower to 5% B for 1 min, giving a total run time of 7 min. The postrun time was 3 min at 5% B. The ion trap mass spectrometer was equipped with an atmospheric pressure electrospray ionization source and was operated in smart mode. Nebulization was achieved with a N_2 pressure of 50 psi, and solvent evaporation assisted by a flow of He drying gas (11 L min^{-1}, 325 °C). Mass spectra were obtained in positive ion mode, and target masses (*m/z*) were set at 603 (TXPTS oxide, **3**), 602 (aza-ylide, **4**), and 892 (*S*-alkylphosphonium adduct, **5**). Retention times and masses of extracted ions were compared to standards on the same instrument. TXPTS oxide (**3**) was prepared by incubating H_2O_2 and TXPTS in a 1:1 molar ratio in H_2O for 5 min. Aza-ylide (**4**) was prepared by incubating hydroxylamine-*O*-sulfonic acid and TXPTS in a 1:1 molar ratio in H_2O for 1 h as previously reported (*41*).

ESI-TOF-MS Analysis. All ESI-TOF MS data was collected on an Agilent MSD TOF system. The operating conditions for MS analysis were as follows: positive ion mode, capillary voltage (VCap) 3500 V, nebulizer gas 30 psig, drying gas 5.0 L min^{-1}; fragmentor 140 V; gas temperature 325 °C. The samples were injected into the ion source using a syringe pump (KD Scientific) and a 250 μL Hamilton syringe connected to the ion probe with a 50 μm ID fused silica capillary. The injection flow rate was 10 μL min^{-1}. The averaged MS spectra were deconvoluted using the Agilent MassHunter Workstation Software vs B.01.03.

Acknowledgment: This work was supported by the National Institutes of Health (R01 HL062198, S.B.K.), (R01 CA136810, C.M.F.), and (R33 CA126659, L.B.P.) and Wake Forest University. The NMR spectrometers used in this work were purchased with partial support from NSF (CHE-9708077) and the North Carolina Biotechnology Center (9703-IDG-1007). We thank Dr. C. S. Day (Wake Forest University) for assistance with X-ray crystallography.

Supporting Information Available: This material is available free of charge *via* the Internet at http://pubs.acs.org.

REFERENCES

1. Davies, M. J., Fu, S., Wang, H., and Dean, R. T. (*1999*) Stable markers of oxidant damage to proteins and their application in the study of human disease, *Free Radical Biol. Med. 27*, 1151–1163.
2. Poole, L. B., Karplus, P. A., and Claiborne, A. (2004) Protein sulfenic acids in redox signaling, *Annu. Rev. Pharmacol. Toxicol. 44*, 325–347.
3. Deem, S., Kim, S. S., Min, J. H., Eveland, R., Moulding, J., Martyr, S., Wang, X., Swenson, E. R., and Gladwin, M. T. (2004) Pulmonary vascular effects of red blood cells containing *S*-nitrosated hemoglobin, *Am. J. Physiol. Heart Circ. Physiol. 287*, H2561–2568.
4. Kobayashi-Miura, M., Shioji, K., Hoshino, Y., Masutani, H., Nakamura, H., and Yodoi, J. (2007) Oxygen sensing and redox signaling: the role of thioredoxin in embryonic development and cardiac diseases, *Am. J. Physiol. Heart Circ. Physiol. 292*, H2040–2050.
5. Haendeler, J., Weiland, U., Zeiher, A. M., and Dimmeler, S. (*1997*) Effects of redox-related congeners of NO on apoptosis and caspase-3 activity, *Nitric Oxide 1*, 282–*293*.
6. Hess, D. T., Matsumoto, A., Kim, S. O., Marshall, H. E., and Stamler, J. S. (2005) Protein *S*-nitrosylation: purview and parameters, *Nat. Rev. Mol. Cell Biol. 6*, 150–166.
7. Hogg, N. (2002) The biochemistry and physiology of *S*-nitrosothiols, *Annu. Rev. Pharmacol. Toxicol. 42*, 585–600.
8. Janssen-Heininger, Y. M., Mossman, B. T., Heintz, N. H., Forman, H. J., Kalyanaraman, B., Finkel, T., Stamler, J. S., Rhee, S. G., and van der Vliet, A. (2008) Redox-based regulation of signal transduction: Principles, pitfalls, and promises, *Free Radical Biol. Med. 45*, 1–17.

9. Crawford, J. H., Chacko, B. K., Pruitt, H. M., Piknova, B., Hogg, N., and Patel, R. P. (2004) Transduction of NO-bioactivity by the red blood cell in sepsis: novel mechanisms of vasodilation during acute inflammatory disease, *Blood 104*, 1375–1382.
10. Martinez-Ruiz, A., and Lamas, S. (2005) Detection and identification of *S*-nitrosylated proteins in endothelial cells, *Methods Enzymol. 396*, 131–139.
11. Padgett, C. M., and Whorton, A. R. (1995) *S*-Nitrosoglutathione reversibly inhibits GAPDH by *S*-nitrosylation, *Am. J. Physiol. 269*, C739–749.
12. Xian, M., Chen, X., Liu, Z., Wang, K., and Wang, P. G. (2000) Inhibition of papain by *S*-nitrosothiols. Formation of mixed disulfides, *J. Biol. Chem. 275*, 20467–20473.
13. Stamler, J. S. (2004) *S*-Nitrosothiols in the blood: roles, amounts, and methods of analysis, *Circ. Res. 94*, 414–417.
14. Jourd'heuil, D., Gray, L., and Grisham, M. B. (2000) *S*-Nitrosothiol formation in blood of lipopolysaccharide-treated rats, *Biochem. Biophys. Res. Commun. 273*, 22–26.
15. Xu, J.-W., Ikeda, K., and Yamori, Y. (2007) Inhibitory effect of polyphenol cyanidin on TNF-α-induced apoptosis through multiple signaling pathways in endothelial cells, *Atherosclerosis 193*, 299–308.
16. Marshall, H. E., and Stamler, J. S. (2001) Inhibition of NF-κB by *S*-nitrosylation, *Biochemistry 40*, 1688–1693.
17. Stamler, J. S., and Hausladen, A. (1998) Oxidative modifications in nitrosative stress, *Nat. Struct. Biol. 5*, 247–249.
18. Forrester, M. T., Foster, M. W., and Stamler, J. S. (2007) Assessment and application of the biotin switch technique for examining protein *S*-nitrosylation under conditions of pharmacologically induced oxidative stress, *J. Biol. Chem. 282*, 13977–13983.
19. Jaffrey, S. R., and Snyder, S. H. (2001) The biotin switch method for the detection of *S*-nitrosylated proteins, *Sci. STKE 2001*, pl1.
20. Doctor, A., Gaston, B., and Kim-Shapiro, D. B. (2006) Detecting physiologic fluctuations in the *S*-nitrosohemoglobin micropopulation: Triiodide versus 3C, *Blood 108*, 3225–3226; author reply 3226–3227.
21. Gow, A., Doctor, A., Mannick, J., and Gaston, B. (2007) *S*-Nitrosothiol measurements in biological systems, *J. Chromatogr., B 851*, 140–151.
22. Xu, X., Cho, M., Spencer, N. Y., Patel, N., Huang, Z., Shields, H., King, S. B., Gladwin, M. T., Hogg, N., and Kim-Shapiro, D. B. (2003) Measurements of nitric oxide on the heme iron and β-93 thiol of human hemoglobin during cycles of oxygenation and deoxygenation, *Proc. Natl. Acad. Sci. U.S.A. 100*, 11303–11308.
23. Park, J. K., and Kostka, P. (1997) Fluorometric detection of biological *S*-nitrosothiols, *Anal. Biochem. 249*, 61–66.
24. Giustarini, D., Dalle-Donne, I., Colombo, R., Milzani, A., and Rossi, R. (2008) Is ascorbate able to reduce disulfide bridges? A cautionary note, *Nitric Oxide 19*, 252–258.
25. Landino, L. M., Koumas, M. T., Mason, C. E., and Alston, J. A. (2006) Ascorbic acid reduction of microtubule protein disulfides and its relevance to protein *S*-nitrosylation assays, *Biochem. Biophys. Res. Commun. 340*, 347–352.
26. Moore, L. R., and Shaughnessy, K. H. (2004) Efficient aqueous-phase Heck and Suzuki couplings of aryl bromides using tri(4,6-dimethyl-3- sulfonatophenyl)phosphine trisodium salt (TXPTS), *Org. Lett. 6*, 225–228.
27. Haake, M. (1972) Zur desoxygenierung von tritylthionitrit, *Tetrahedron Lett. 13*, 33–39.
28. Wang, H., Zhang, J., and Xian, M. (2009) Facile formation of dehydroalanine from *S*-nitrosocysteines, *J. Am. Chem. Soc. 131*, 13238–13239.
29. Zhang, J., Wang, H., and Xian, M. (2009) Exploration of the "traceless" reductive ligation of *S*-nitrosothiols, *Org. Lett. 11*, 477–480.
30. Wang, H., and Xian, M. (2008) Fast reductive ligation of *S*-nitrosothiols, *Angew. Chem., Int. Ed. 47*, 6598–6601.
31. Saxon, E., and Bertozzi, C. R. (2000) Cell surface engineering by a modified Staudinger reaction, *Science 287*, 2007–2010.
32. Langer, R., Shi, W., and Rothenberger, A. (2006) Copper-mediated cleavage of disulfides by tertiary phosphines: A new route to As-S anions, *Dalton Trans. 37*, 4435–4437.
33. Valeriy, E. P., Alexei, V. B., and Yuriy, G. S. (2008) Comparison of the reactivity of *N*-(*p*-toluenesulfonyl)-sulfinimidoyl fluorides and chlorides toward triphenylphosphine, *Heteroat. Chem. 19*, 66–71.
34. Omelanczuk, J., and Mikolajczyk, M. (1979) Optically active trivalent phosphorus compounds. 2. Reactivity of alkylthio- and alkylselenophosphonium salts. The first stereospecific synthesis of a chiral phosphinite, *J. Am. Chem. Soc. 101*, 7292–7295.
35. Cline, D. J., Redding, S. E., Brohawn, S. G., Psathas, J. N., Schneider, J. P., and Thorpe, C. (2004) New water-soluble phosphines as reductants of peptide and protein disulfide bonds: reactivity and membrane permeability, *Biochemistry 43*, 15195–15203.
36. Han, J. C., and Han, G. Y. (1994) A procedure for quantitative determination of tris(2-carboxyethyl)phosphine, an odorless reducing agent more stable and effective than dithiothreitol, *Anal. Biochem. 220*, 5–10.
37. Overman, L. E., Matzinger, D., O'Connor, E. M., and Overman, J. D. (1974) Nucleophilic cleavage of the sulfur-sulfur bond by phosphorus nucleophiles. Kinetic study of the reduction of aryl disulfides with triphenylphosphine and water, *J. Am. Chem. Soc. 96*, 6081–6089.
38. Houk, J., Singh, R., and Whitesides, G. M. (1987) Measurement of thiol-disulfide interchange reactions and thiol pK_a values, *Methods Enzymol. 143*, 129–140.
39. Poole, L. B., and Ellis, H. R. (2002) Identification of cysteine sulfenic acid in AhpC of alkyl hydroperoxide reductase, *Methods Enzymol. 348*, 122–136.
40. Nelson, K. J., Parsonage, D., Hall, A., Karplus, P. A., and Poole, L. B. (2008) Cysteine pK_a values for the bacterial peroxiredoxin AhpC, *Biochemistry 47*, 12860–12868.
41. Reisz, J. A., Klorig, E. B., Wright, M. W., and King, S. B. (2009) Reductive phosphine-mediated ligation of nitroxyl (HNO), *Org. Lett. 11*, 2719–2721.
42. Liu, L., Hausladen, A., Zeng, M., Que, L., Heitman, J., and Stamler, J. S. (2001) A metabolic enzyme for *S*-nitrosothiol conserved from bacteria to humans, *Nature 410*, 490–494.
43. Jensen, D. E., Belka, G. K., and Du Bois, G. C. (1998) *S*-Nitrosoglutathione is a substrate for rat alcohol dehydrogenase class III isoenzyme, *Biochem. J. 331*, (Pt 2), 659–668.
44. Lecher, H., and Siefken, W. (1926) Nitrosyl derivatives of bivalent sulfur. II. Nitrosyl ethyl mercaptide. II, *Chem. Ber. 59*, 2594–2601.
45. Hart, T. W. (1985) Some observations concerning the *S*-nitroso and *S*-phenylsulphonyl derivatives of L-cysteine and glutathione, *Tetrahedron Lett. 26*, 2013–2016.
46. Poole, L. B., and Ellis, H. R. (1996) Flavin-dependent alkyl hydroperoxide reductase from *Salmonella typhimurium*. 1. Purification and enzymatic activities of overexpressed AhpF and AhpC proteins, *Biochemistry 35*, 56–64.